



Journals & books

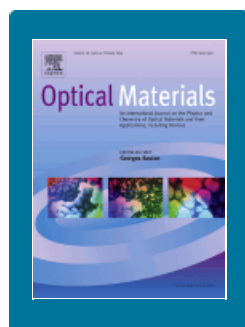
Online tools

Authors, editors & reviewers

About Elsevier

Community

Store



Optical Materials

Guide for Authors

Submit Your Paper

Track Your Paper

Order Journal

View Articles

Open Access Options

Most Downloaded
ArticlesRecent Open Access
Articles

News

Most Cited Articles

Special Issues

Recent Articles

Stay up-to-date

Register your interests
and receive email alerts
tailored to your needs[Click here to sign up](#)

Follow us



Most Cited Optical Materials Articles

The most cited articles published since 2009, extracted from [Scopus](#).[Properties of transparent Ce:YAG ceramic phosphors for white LED](#)Volume 33, Issue 5, March 2011, Pages 688-691
Nishiura, S. | Tanabe, S. | Fujioka, K. | Fujimoto, Y.

Transparent Ce:YAG ceramic phosphors were synthesized from the oxide powder which was produced by co-preparation method of the hydroxides. The Ce:YAG ceramics had a broad emission band peaked at 530 nm due to the 5d → 4f transition of Ce³⁺. The transmittances of the samples obtained were 70-87% at 800 nm. The absorption coefficient and emission intensity of Ce³⁺ were increased with increasing thickness. Under 465 nm LED excitation, the color coordinates of the Ce:YAG ceramics shifted from the blue region to yellow region with increasing sample thickness, passing nearby the theoretical white point in the chromaticity diagram. The highest value of luminous efficacy of the ceramic white LED was 73.5 lm/W. © 2010 Elsevier B.V. All rights reserved.

Share Article

[A review on the light extraction techniques in organic electroluminescent devices](#)Volume 32, Issue 1, November 2009, Pages 221-233
Saxena, K. | Jain, V.K. | Mehta, D.S.

Organic electroluminescent devices are becoming increasingly important because of their potential applications for large area flat-panel displays and general lighting. The internal quantum efficiency of these devices have been achieved near 100% using electro-phosphorescent materials with proper management of singlet and triplet excitons, however, the external quantum efficiency of conventional devices remains near 20% because of losses due to wave-guiding effect. Recently, there has been great progress to enhance the light out-coupling efficiency of organic electroluminescent devices by means of various internal and external device modification techniques. In this review we report recent advances in light out-coupling techniques, such as, substrate modification methods, use of scattering medium, micro-lens arrays, micro-cavity effect, photonic crystals and nano-cavity, nano-particles, nano-structures and surface plasmon-enhanced techniques that have been implemented to enhance the external extraction efficiency of organic electroluminescent devices. © 2009 Elsevier B.V. All rights reserved.

Share Article

[Preparation, characterization, and strong upconversion of monodisperse Y2O3:Er3+,Yb3+ microspheres](#)Volume 31, Issue 4, February 2009, Pages 583-589
Guo, H. | Qiao, Y.M.

Monodisperse Y2O3:Er and Y2O3:Er,Yb microspheres with diameter of 1.5-3 μm, which are composed of nanoparticles with size of about 50 nm, were prepared by a simple solvothermal method followed by further heat treatment. The structural properties of samples were investigated by X-ray diffraction; field emission scanning electron microscopy, Raman spectroscopy and Fourier transform infrared spectroscopy. Especially, the effect of CH3COONa on the formation of microspheres was investigated. Under 980 nm laser excitation, strong green (518-570 nm), strong red (645-686 nm) and weak violet (405-420 nm) upconversion emissions have been observed in Y2O3:Er and Y2O3:Er,Yb microspheres. The upconversion mechanisms were studied through laser power and concentration dependence of the upconverted emissions. The upconversion properties indicate that Y2O3:Er and Y2O3:Er,Yb microspheres may be used in upconversion phosphors. © 2008 Elsevier B.V. All rights reserved.

Share Article

[Uniform YVO4:Ln3+ \(Ln = Eu, Dy, and Sm\) nanocrystals: Solvothermal synthesis and luminescence properties](#)Volume 31, Issue 6, April 2009, Pages 1032-1037
Jia, G. | Song, Y. | Yang, M. | Huang, Y. | Zhang, L. | You, H.

Well-dispersed YVO4:Ln³⁺ (Ln = Eu, Dy, and Sm) nanocrystals with uniform morphology and size have been synthesized via a facile solvothermal route. XRD results demonstrate that all of the three samples can be well indexed to the pure tetragonal phase of YVO4, indicating that the Eu³⁺, Dy³⁺, and Sm³⁺ have been

effectively doped into the host lattices of YVO₄. TEM images show that the YVO₄ nanocrystals exhibit ellipsoid shape and a mean size of about 20 nm, which is in good agreement with the estimation of XRD results. The YVO₄:Ln³⁺ (Ln = Eu, Dy, and Sm) nanocrystals show strong light emissions with different colors coming from different Ln³⁺ ions under ultraviolet excitation or low-voltage electron beams excitation, which might find potential applications in the fields such as light emitting phosphors, advanced flat panel display, field emission display devices or biological labeling. © 2008 Elsevier B.V. All rights reserved.

Share Article



Influence of doping concentrations on the aluminum doped zinc oxide thin films properties for ultraviolet photoconductive sensor applications

Volume 32, Issue 6, April 2010, Pages 696-699

Mamat, M.H. | Sahdan, M.Z. | Khusaimi, Z. | Ahmed, A.Z. | Abdullah, S. | Rusop, M.

Aluminum (Al) doped zinc oxide (ZnO) thin films have been prepared on microscope glass substrate using sol-gel spin-coating method with different doping concentrations from 0 to 3 at.%. The thin films were characterized using X-ray diffractometer (XRD), UV-vis-NIR spectrophotometer, Current-Voltage (I-V) measurement system and photocurrent measurement system for applications in ultraviolet (UV) photoconductive sensor. From the XRD analysis, increasing of doping concentration affected structural properties of the thin film where c-axis orientation becomes weaker. UV-vis-NIR spectra reveals all films exhibit high transmission (>80%) in UV-NIR region. Improvement in electrical properties with dopant concentrations is observed as shown by I-V measurement results. 1 at.% Al doped ZnO thin film shows the highest photocurrent value after irradiated with UV lamp (365 nm). © 2009 Elsevier B.V. All rights reserved.

Share Article



Transparent compact ceramics: Inherent physical issues

Volume 31, Issue 8, June 2009, Pages 1144-1150

Krell, A. | Klimke, J. | Hutzler, T.

The overview focuses on inherent optical properties, governed by composition and the state of the crystal lattice, and on the interference of these properties with the microstructural optimization of transparent ceramics (e.g. the dependence of the tolerable pore size or grain size on the refractive index). Starting with the general difference between the dispersive performances $n(\lambda)$ of glasses and transparent ceramics, examples will demonstrate the use of compositional changes for tuning the relationship of index, Abbe number, and anomalous dispersion. Perovskites and cubic zirconia are known candidates for such developments, but their mechanical strength is low. Therefore, physical conditions are investigated for bringing translucent tetragonal ZrO₂ to transparency. Another field of increasing interest is transparency at extreme wave lengths affected by point defects, associated absorption and scattering mechanisms. © 2008 Elsevier B.V. All rights reserved.

Share Article



Lanthanide level location in transition metal complex compounds

Volume 32, Issue 12, October 2010, Pages 1681-1685

Dorenbos, P. | Krumpel, A.H. | Van Der Kolk, E. | Boutinaud, P. | Bettinelli, M. | Cavalli, E.

We will provide a method to place the levels of all trivalent lanthanides with respect to the top of the valence band and bottom of the conduction band in oxides containing transition metal complexes. The method will be applied to CaTiO₃, YVO₄, LaVO₄, CaNb₂O₆, YNbO₄, CaWO₄, YTaO₄, and LaTaO₄, but in principle can be applied to any oxide containing transition metal complexes with lanthanide dopants on either rare earth or alkaline earth sites. Crucial to place the energy levels is the energy for intervalence charge transfer between a lanthanide (Pr³⁺ and Tb³⁺) and a transition metal ion (Ti⁴⁺, V⁵⁺, Nb⁵⁺, Mo⁶⁺, Ta⁵⁺, W⁶⁺) that can be observed in luminescence excitation spectra. The quenching of Pr³⁺ emission from the ³P₀ state and of Tb³⁺ emission from the ⁵D₃ and ⁵D₄ states provides complementary information. © 2010 Elsevier B.V. All rights reserved.

Share Article



Judd-Ofelt parameters and radiative properties of Sm³⁺ ions doped zinc bismuth borate glasses

Volume 32, Issue 2, December 2009, Pages 339-344

Agarwal, A. | Pal, I. | Sanghi, S. | Aggarwal, M.P.

Glasses having composition 20ZnO·xBi₂O₃·(79-x)B₂O₃ (15 ≤ x ≤ 35 mol%) and doped with 1 mol% Sm³⁺ ions have been prepared by melt quench technique. Optical absorption and fluorescence spectra have been recorded. Judd-Ofelt approach has been applied for the f ↔ f transition of Sm³⁺ ions to evaluate various intensity parameters (Ω₂, Ω₄, Ω₆). The variations in intensity parameters, radiative transition probabilities and hypersensitive band positions with composition have been discussed. The variation of Ω₂ with Bi₂O₃ content have been attributed to change in the asymmetry of the ligand field at the rare earth ion site and to the changes in their rare earth-oxygen (RE-O) covalency, whereas the variation of Ω₆ is found to be strongly dependent on nephelauxetic effect. The shift of the hypersensitive band shows that the covalency of the RE-O bond increases with increase of Bi₂O₃ content due to increased interaction between the Sm³⁺ ion and non-

bridging oxygens. The radiative transition probabilities for the Sm³⁺ ions are large in zinc bismuth borate glasses, suggesting their suitability as laser material. © 2009 Elsevier B.V. All rights reserved.

Share Article



Optical properties of Pr³⁺, Sm³⁺ and Er³⁺ doped P₂O₅-CaO-SrO-BaO phosphate glass

Volume 32, Issue 4, February 2010, Pages 547-553

Mazurak, Z. | Bodył, S. | Lisiecki, R. | Gabryś-Pisarska, J. | Czaja, M.

In this paper, we present the photoluminescence properties of Pr³⁺, Sm³⁺ and Er³⁺ doped phosphate glasses. Optical absorption and emission spectra of lanthanide active ions in P₂O₅-CaO-SrO-BaO glass have been investigated at room temperature. These glasses have shown strong absorption bands in the near-infrared (NIR) and visible (VIS) region. For Pr³⁺ doped glass, emission bands centered at 608 nm (3P₀ → 3H₆ + 1D₂ - 3H₄), 640 nm (3P₀ → 3F₂), 686 nm (3P₀-3F₃) and 723 nm (3P₀ → 3F₄) have been observed with 480 nm (3H₄ → 3P₀) excitation wavelength. Of them, 686 nm has shown bright red emission. Emission bands of (4G_{5/2} → 6H_{5/2}) 560 nm, (4G_{5/2} → 6H_{7/2}) 600 nm and (4G_{5/2} → 6H_{9/2}) 645 nm for the Sm³⁺ phosphate glass, with excitation at (6H_{5/2} → 4F_{7/2}) 400 nm have been recorded. With regard to the Er³⁺ phosphate glass, a bright fluorescent green-yellow emission at 546 nm (4S_{3/2} → 4I_{15/2}) have been observed. Analysis of decay curves of luminescence revealed occurrence of the strong luminescence quenching originating from the 3P₀ metastable level of Pr³⁺ and 4S_{3/2} state of Er³⁺ mainly by a multiphonon relaxation processes to 1D₂, 4F_{9/2} levels respectively. Moreover these results are compared with those obtained by using the Judd-Ofelt theory. According to the Judd-Ofelt theory, the Judd-Ofelt intensity parameters Ω_{2,4,6} were calculated, by which the radiative transition probabilities and radiative lifetimes of luminescent levels were obtained. © 2009 Elsevier B.V. All rights reserved.

Share Article



Optical properties of Dy³⁺-doped phosphate and fluorophosphate glasses

Volume 31, Issue 4, February 2009, Pages 624-631

Babu, S.S. | Babu, P. | Jayasankar, C.K. | Tröster, Th. | Sievers, W. | Wortmann, G.

Optical properties of Dy³⁺-doped phosphate (P₂O₅ + K₂O + BaO + Al₂O₃) and fluorophosphate (P₂O₅ + K₂O + BaO + BaF₂ + Al₂O₃) glasses have been investigated. The observed bands in absorption spectra of 1.0 mol% Dy³⁺-doped glasses have been assigned and analyzed using the parametric free-ion Hamiltonian model. Judd-Ofelt (JO) intensity parameters have been obtained from the optical absorption spectra. The sensitiveness of the Ω₂ JO parameter to the hypersensitive transition has been demonstrated. Using these JO parameters radiative properties of some of the excited states of Dy³⁺ ions have been calculated. A strong yellow emission was observed from the 4F_{9/2} → 6H_{13/2} transition of Dy³⁺ ions in these glasses. The peak stimulated emission cross-section for the 4F_{9/2} → 6H_{13/2} transition is found to be comparable with those of other Dy³⁺ systems. The decay curves of the 4F_{9/2} level have been measured and are found to deviate from exponential nature with increase in Dy³⁺ ions concentration. The non-exponential decay curves have been fitted with the Inokuti-Hirayama model which revealed that dipole-dipole mechanism is responsible for the energy transfer processes through Dy³⁺-Dy³⁺ interactions. © 2008 Elsevier B.V. All rights reserved.

Share Article



New developments in luminescence for solar energy utilization

Volume 32, Issue 9, July 2010, Pages 850-856

Reisfeld, R.

As our fossil sources of energy diminish constantly search for alternative energy solutions becomes vital. The interest in exploiting solar energy for photovoltaic electricity has grown exponentially in recent decade, however, its high cost is still a limiting factor for massive uses. Static luminescent concentrator could provide a partial solution if properly designed. The paper summarizes the requirements for efficient and photostable luminescent concentrators, provides the latest results and ideas and shows how they can be materialized. It is demonstrated how the plate efficiency can be improved by applying a thin film with optical contact to transparent plate, silver plasmons that increase the transition probability of the colorants, photonic systems preventing the escape of the luminescence from the plate when traveling to the cell, creating fluorescence in the UV and visible part of the spectrum, using materials in which the absorption and emission from different electronic levels prevent self-absorption. © 2010 Elsevier B.V. All rights reserved.

Share Article



Near-infrared quantum cutting in Ce³⁺, Yb³⁺ co-doped YBO₃ phosphors by cooperative energy transfer

Volume 32, Issue 9, July 2010, Pages 998-1001

Chen, J. | Guo, H. | Li, Z. | Zhang, H. | Zhuang, Y.

An efficient near-infrared (NIR) quantum cutting (QC) in Ce³⁺, Yb³⁺ co-doped YBO₃ phosphors has been demonstrated, which involves the emission of two low-energy NIR photons (around 973 nm) from an absorbed ultra-violet (UV) photon at 358 nm via a cooperative energy transfer (CET) from Ce³⁺ to Yb³⁺ ions. Yb³⁺ concentration dependent quantum efficiency has been calculated and the maximum efficiency approaches up to 175% before reaching the critical concentration quenching threshold. The development of NIR QC Ce³⁺, Yb³⁺ co-doped phosphors may open up a new approach to achieve high efficiency silicon-

based solar cells by means of downconversion. © 2010 Elsevier B.V. All rights reserved.

Share Article



A detailed study on the requirements for angular homogeneity of phosphor converted high power white LED light sources

Volume 31, Issue 6, April 2009, Pages 837-848

Sommer, C. | Hartmann, P. | Pachler, P. | Schweighart, M. | Tasch, S. | Leising, G. | Wenzl, F.P.

We present a simulation procedure based on optical ray-tracing in order to optimize the angular homogeneity of the light emitted from the color conversion element (CCE) in a phosphor conversion-based white LED. The blue LED and the yellow CCE light have rather different emission characteristics; so the geometry of the CCE as well as its phosphor concentration have to be carefully adjusted in order to achieve equal irradiance and/or radiant intensity distributions on a photo-detector surrounding the LED. The simulations identify the optimal CCE geometries and material compositions in order to obtain angular homogeneity for a broad range of color temperatures. © 2008 Elsevier B.V. All rights reserved.

Share Article



Red phosphor SrWO₄:Eu³⁺ for potential application in white LED

Volume 33, Issue 6, April 2011, Pages 909-913

Ju, Z. | Wei, R. | Gao, X. | Liu, W. | Pang, C.

A series of red light emissive phosphors Sr_{1-x}WO₄:Eu³⁺ (x = 0.02-0.10) and Sr_{0.84}WO₄:Eu_{0.083}⁺, M_{0.08}⁺ (M = Li, Na, K) were prepared through solid-state reactions, and their luminescent properties were studied. The influences of contents of Eu³⁺ and charge compensators on the luminescent properties were discussed. Both the fluorescent intensities and quantum yields are greatly improved through adding charge compensators. The phosphors can be effectively excited by the light of 394 and 465 nm, and show bright red emissions. The decay curves are well fitted with single exponential decay models. Furthermore, the temperature-dependent luminescence indicates the phosphors exhibit small thermal-quenching properties. So the phosphors are able to be applied to white light-emitting diodes. © 2011 Elsevier B.V. All rights reserved.

Share Article



White emission using mixtures of CdSe quantum dots and PMMA as a phosphor

Volume 32, Issue 4, February 2010, Pages 515-521

Chung, W. | Park, K. | Yu, H.J. | Kim, J. | Chun, B.-H. | Kim, S.H.

White light emitting diodes (LEDs) were fabricated using an InGaN 460 nm blue emission LED chip as the excitation source and CdSe quantum dots dispersed in PMMA as the phosphor. CdSe quantum dots were synthesized by the wet chemical method using CdO and Selenium powder as precursors. The three different size, 2.9, 3.4 and 4.3 nm in diameter, of CdSe quantum dots obtained using this method exhibited emission peaks at 555, 580 and 625 nm, respectively with a quantum yield of 10-30%. Mixed phosphors containing different weight ratio of CdSe and PMMA (1:0.1, 1:1, 1:5 and 1:10 wt%) were deposited on the LED chip to investigate the effects of different weight ratios of CdSe and PMMA on the performance of the white LEDs. The fabricated white LEDs that contained CdSe and PMMA weight ratio at 1:10 showed the best performance and the CIE color coordinates varied less with different applied currents. The luminous efficiency of single phosphor (580 nm CdSe) white LEDs was 5.62 lm/W with a CRI of 15.7, whereas the luminous efficiency of dual phosphors (555, 625 nm CdSe) white LEDs was 3.79 lm/W with a CRI of 61.4 at 20 mA. The CIE coordinates of single and dual phosphors white LEDs varied from (0.33, 0.28) to (0.29, 0.26) and from (0.39, 0.33) to (0.39, 0.32), respectively, when the working current ranged from 5 to 80 mA. © 2009 Elsevier B.V. All rights reserved.

Share Article



Spectroscopic study of Dy³⁺ and Dy³⁺/Yb³⁺ ions co-doped in barium fluoroborate glass

Volume 31, Issue 10, August 2009, Pages 1472-1477

Dwivedi, Y. | Rai, S.B.

Dy³⁺ and Dy³⁺/Yb³⁺ co-doped barium fluoroborate glasses have been synthesized and their luminescence properties have been monitored under UV (355 nm) and NIR (976 nm) excitations, respectively. Absorption spectra of the two samples were recorded and Judd-Ofelt intensity parameters and other radiative parameters were calculated and compared. Dy³⁺ doped sample yields strong yellowish white emission under 355 nm excitation. No emission is observed with 976 nm excitation. The Dy³⁺/Yb³⁺ ions co-doped sample on the other hand gives weak upconversion emission in blue, yellow and red regions on 976 nm excitation via energy transfer process from Yb³⁺ to Dy³⁺ ions from other level. An involvement of three photons has been noted for these emissions. Decay curve for different transitions of these samples have also been recorded and the lifetime of the corresponding levels involved are calculated. © 2009 Elsevier B.V. All rights reserved.

Share Article



Upconversion color tunability and white light generation in Tm³⁺/Ho³⁺/Yb³⁺ doped aluminum germanate glasses

Volume 32, Issue 4, February 2010, Pages 554-559

Gong, H. | Yang, D. | Zhao, X. | Yun Bun Pun, E. | Lin, H.

Tm³⁺/Ho³⁺/Yb³⁺ triply doped aluminum germanate glasses exhibiting multicolor upconversion fluorescences have been fabricated and characterized. Efficient three-photon blue upconversion emission of Tm³⁺ and two-photon green and red upconversion fluorescences of Ho³⁺ have been observed. The strong red emission of Ho³⁺, which is more than eight times higher than that of the green emission, is desirable in achieving high color rendering index. By varying the excitation power of the 974 nm wavelength laser diode, a series of white fluorescences with a large range of correlated color temperature (CCT) was obtained, and the fluorescence colors can be tuned from yellowish white to warm white, pure white, cool white, and bluish white with different CCT. The upconversion color tunability via pump power adjustment will promote the development of three-dimensional solid-state displays and upconversion illumination devices. © 2009 Elsevier B.V. All rights reserved.

Share Article



Effect of optical basicity on broadband infrared fluorescence in bismuth-doped alkali metal germanate glasses

Volume 31, Issue 6, April 2009, Pages 945-948

Chi, G. | Zhou, D. | Song, Z. | Qiu, J.

Bismuth-doped alkaline metal germanate glasses with infrared fluorescence covering the whole low loss wavelength region were developed. The infrared fluorescence centered around 1.31 μm with the full width at half maximum (FWHM) larger than 200 nm was observed in GeO₂-R₂O-Bi₂O₃ (R = Li, Na, K) glasses under an 808 nm LD excitation, whereby the fluorescence lifetime is longer than 400 μs. These results indicate that the glass material may have potential applications in broadband optical amplifiers. The intensity of the infrared fluorescence decreases with the increase in the optical basicity of the host glasses. It is suggested that the fluorescence in the near infrared region should be ascribed to the low valence state of bismuth such as Bi²⁺ or Bi⁺, because a higher optical basicity favors the higher valence state of the multivalence metal ions. © 2008 Elsevier B.V. All rights reserved.

Share Article



Synthesis and optical characterizations of Yb-doped CaF₂ ceramics

Volume 31, Issue 5, March 2009, Pages 750-753

Aubry, P. | Bensalah, A. | Gredin, P. | Patriarche, G. | Vivien, D. | Mortier, M.

Nanopowders of Yb-doped calcium fluoride were obtained by three different ways: mechanical alloying, reverse micelle method and co-precipitation. Transmission electron microscopy showed that the particle sizes were monodispersed for the powders obtained from soft chemistry with an average size around 20 nm and polydispersed for the powder from the chemical alloying. An annealing step at 400 °C is needed to remove impurities adsorbed at the particles surface for powders obtained from the reverse micellar and the co-precipitation methods. Transparent ceramic with a grain mean size of 24 μm was obtained from the co-precipitation synthesized powder after a vacuum sintering followed by a HIP post-treatment. Loss of transmission can be attributed mainly to the presence of a residual closed porosity. The best transmission value is 55% reached in the infrared range at 1.2 μm. © 2008 Elsevier B.V. All rights reserved.

Share Article



Crystal growth, optical properties, and α-ray responses of Ce-doped LiCaAlF₆ for different Ce concentration

Volume 32, Issue 2, December 2009, Pages 311-314

Yanagida, T. | Yoshikawa, A. | Yokota, Y. | Maeo, S. | Kawaguchi, N. | Ishizu, S. | Fukuda, K. | Suyama, T.

Ce 1%, 2%, and 3%-doped LiCaAlF₆ (LiCAF) single crystals were grown by the micro-pulling-down method. The crystals were transparent, 2.0 mm in diameter and 30-60 mm in length. Neither visible inclusions nor cracks were observed. Optical properties, including absorption coefficient, and photoluminescence emission spectra were measured. The strong absorption line was observed at 260 nm, and absorption coefficients of this line were proportional to Ce³⁺ concentration. Emission due to Ce³⁺ 5d-4f transition peaking around 285 nm and 310 nm were observed by 260 nm excitation. Simulating a neutron irradiation, 241Am 5.5 MeV α-ray was used to excite the samples. After a correction of a quantum efficiency of photomultiplier tube and compared with Li-glass scintillator GS20, light yield of 6600 ph/n, and 41 ns decay were achieved 3% doped. © 2009 Elsevier B.V. All rights reserved.

Share Article



Upconversion luminescence of transparent Er³⁺-doped chalcogenide glass-ceramics

Volume 31, Issue 5, March 2009, Pages 760-764

Balda, R. | García-Revilla, S. | Fernández, J. | Seznec, V. | Nazabal, V. | Zhang, X.H. | Adam, J.L. | Allix, M. | Matzen, G.

Upconversion luminescence of Er³⁺ ions in chalcogenide glass and in transparent glass-ceramic samples under continuous wave and pulsed laser excitation in the 4I_{9/2} level has been studied. Green and red

emissions corresponding to $(2H_{11/2}, 4S_{3/2}) \rightarrow 4I_{15/2}$ and $4F_{9/2} \rightarrow 4I_{15/2}$ transitions, respectively, have been observed and attributed to a two photon upconversion process. A significant increase of upconversion luminescence has been observed in the transparent glass-ceramics if compared with the one from the base glass. Moreover, the red emission corresponding to the $4F_{9/2} \rightarrow 4I_{15/2}$ transition is enhanced in the glass-ceramics as compared to the green luminescence from $(2H_{11/2}, 4S_{3/2})$ levels probably due to an increase of the energy transfer processes populating the $4F_{9/2}$ level. The possible excitation mechanisms responsible for this upconversion luminescence are discussed. © 2008 Elsevier B.V. All rights reserved.

Share Article



Basic study of Europium doped LiCaAlF₆ scintillator and its capability for thermal neutron imaging application

Volume 33, Issue 8, June 2011, Pages 1243-1247

Yanagida, T. | Kawaguchi, N. | Fujimoto, Y. | Fukuda, K. | Yokota, Y. | Yamazaki, A. | Watanabe, K. | Pejchal, J. | Uritani, A. | Iguchi, T. | Yoshikawa, A.

Eu²⁺ 0.1, 0.5, 1, and 2 mol% doped LiCaAlF₆ single crystalline scintillators were grown by the micro-pulling down (μ -PD) method. Eu²⁺ 2 mol% doped LiCaAlF₆ was also prepared using the Czochralski method. In the transmittance spectra, 4f-5d absorption lines appeared around 200-220 and 290-350 nm. An intense emission at 375 nm due to Eu²⁺ 5d-4f transition was observed under ²⁴¹Am α -ray excitation. When ²⁵²Cf excited pulse height spectra were measured, Eu 2% doped one showed the highest light yield of 29,000 ph/n with 1.15 μ s decay time. Using the 2 inch Czochralski grown one coupled with the position sensitive photomultiplier tube covered by Cd mask with various size (1, 2, 3, and 5 mm) pin holes, thermal neutron imaging was examined. As a result, the spatial resolution turned out to be better than 1 mm. © 2011 Elsevier B.V. All rights reserved.

Share Article



Optimization and kinetics of electroless Ni-P-B plating of quartz optical fiber

Volume 31, Issue 10, August 2009, Pages 1532-1539

Jiang, B. | Xiao, L. | Hu, S. | Peng, J. | Zhang, H. | Wang, M.

The preparation of Ni-P-B coatings on surface of quartz optical fibers was carried out using electroless plating method. The effects of the concentrations of nickel chloride, sodium hypophosphite, potassium borohydride, ethylenediamine, cadmium sulfate and temperature on the quality of Ni-P-B coatings were investigated by orthogonal experiment and their optimal values were determined to be: 0.1 mol L⁻¹, 0.094 mol L⁻¹, 0.185 mol L⁻¹, 0.36 mol L⁻¹, 5.68×10^{-4} mol L⁻¹ and 90 °C, respectively. The effect of coarsening time of the naked fiber on the quality of Ni-P-B coatings was also researched and the optimal coarsening time was determined to be 15 min. Stereomicroscope, Scanning Electron Microscope and X-ray diffractometer were used to characterize the apparentness, morphology and structure of the prepared Ni-P-B coatings. Inductively Coupled Plasma-Atomic Emission Spectroscopy, Thermal Shock Method and Gravimetric Analysis Method were employed to analyze the composition, force of adhesion and solderability of the coatings, respectively. The results showed that a Ni-P-B coating with low surface roughness, good strength of adhesion, low resistivity and good solderability was successfully prepared. The kinetic models (Ni-P-B deposition rate equations) of the process were established as $v = 7.95 \times 10^{-6} \text{ cA } 0.830 \text{ cB } 0.428 \text{ cC } - 0.288 \text{ cD } - 0.645 \text{ cE } 0.02 \exp \frac{26788}{T - 298}$, 298 RT; $v = 1.03 \times 10^{-7} \text{ cA } 0.830 \text{ cB } 0.428 \text{ cC } - 0.288 \text{ cD } - 0.645 \text{ cE } - 0.614 \exp \frac{26788}{T - 298}$, 298 RT). The theoretical values calculated by the models were proved to be basically consistent with the practical measurements through experimental verification. © 2009 Elsevier B.V. All rights reserved.

Share Article



Absorption and fluorescence properties of Sm³⁺ ions in fluoride containing phosphate glasses

Volume 31, Issue 8, June 2009, Pages 1167-1172

Suhasini, T. | Suresh Kumar, J. | Sasikala, T. | Jang, K. | Lee, H.S. | Jayasimhadri, M. | Jeong, J.H. | Yi, S.S. | Rama Moorthy, L.

Optical absorption, fluorescence and lifetime characteristics of Sm³⁺-doped fluoride containing phosphate glasses (PKFBASm) with molar composition of $(56-x/2) \text{ P}_2\text{O}_5 + 14 \text{ K}_2\text{O} + 6\text{KF} + (15-x/2) \text{ BaO} + 9\text{Al}_2\text{O}_3 + x \text{ Sm}_2\text{O}_3$, ($x = 0.01, 0.05, 0.1, 1.0, 2.0, 4.0$ and 6.0 mol%) were studied. From the measured energies of absorption bands, different free-ion energy level parameters along with calculated energies were determined using the free-ion Hamiltonian (HFI) model. Judd-Ofelt (J-O) theory was applied to the experimental oscillator strengths to evaluate three phenomenological J-O intensity parameters Ω_λ ($\lambda = 2, 4$ and 6). Using these J-O parameters as well as from the emission and decay measurements, various radiative parameters such as transition probabilities (AR), radiative lifetimes (τ_R), measured lifetimes (τ_{mes}), calculated branching ratios (β_R), measured branching ratios (β_{mes}), effective bandwidths ($\Delta\lambda_{\text{eff}}$) and stimulated emission cross-sections (σ_{sp}) have been calculated for the excited 4G_{5/2} luminescent level. The nature of decay curves of 4G_{5/2} level for different Sm³⁺ ion concentrations in all PKFBASm glasses has been analyzed using Inokuti-Hirayama (I-H) model and the lifetimes are noticed to decrease with increase of concentration. The cross-relaxation mechanism responsible for the quenching of measured lifetimes with concentration is also discussed. © 2009 Elsevier B.V. All rights reserved.

Share Article



Share Article



Fabrication and characterization of rhombic silver nanoparticles for biosensing

Volume 31, Issue 6, April 2009, Pages 769-774

Zhu, S. | Du, C. | Fu, Y.

Fabrication and characterization of rhombic silver nanoparticles array being used as a localized surface plasmon resonance (LSPR)-based nano-biosensor were reported in this paper. The sensor consists of a rhombic Ag nanoparticles array with single particle dimension of ~140 nm in-plane width and 47 nm out-of-plane height. Characteristics of the nanoparticles such as extinction spectroscopy properties, refractive index sensitivity, and concentration of the target molecules were analyzed. The LSPR-based extinction spectra of the antigen or antibody with lower concentration were detected. The detection results from 100 nM target molecule indicate a larger peak wavelength shift for the rhombic nanoparticles-based nano-biosensor than that of the reported triangular particles-based biosensor. Using a discrete dipole approximation (DDA) algorithm aided design approach we demonstrated that the refractive index sensitivity is 330 nm per refractive index unit for the fabricated rhombic Ag nanoparticles array. © 2008 Elsevier B.V. All rights reserved.

Share Article



Share this page:



ADVERTISEMENT

CELEBRATING
RESEARCH
EXCELLENCE

Visit the new
global awards
website



- | | | | | | | |
|---|--|--|--|--|--|------------------|
| <p>Readers</p> <ul style="list-style-type: none"> View Articles Volume/ Issue Alert | <p>Authors</p> <ul style="list-style-type: none"> Author Information Pack Submit Your Paper Track Your Paper Webshop | <p>Librarians</p> <ul style="list-style-type: none"> Ordering Information and Dispatch Dates Abstracting/ Indexing | <p>Editors</p> <ul style="list-style-type: none"> Publishing Ethics Resource Kit EES Support | <p>Reviewers</p> <ul style="list-style-type: none"> Reviewer Guidelines Log in as Reviewer | <p>Advertisers/ Sponsors</p> <ul style="list-style-type: none"> Advertisers Media Information | <p>Societies</p> |
|---|--|--|--|--|--|------------------|



Cookies are set by this site. To decline them or learn more, visit our [Cookies](#) page.